Rare Metal Materials and Engineering
Volume 51, Issue 4, April 2022
Available online at www.rmme.ac.cn

Science Press

Cite this article as: Li Zhendong, Zhan Hua, Xu Tianyang, et al. Influence of Cr Interlayer Thickness on Residual Stress and Adhesion of Cr-DLC Multilayer Structure Films[J]. Rare Metal Materials and Engineering, 2022, 51(04): 1195-1202.

ARTICLE

Influence of Cr Interlayer Thickness on Residual Stress and Adhesion of Cr-DLC Multilayer Structure Films

Li Zhendong[1,2], Zhan Hua[1,2], Xu Tianyang[1,2], Bao Manyu[1,2], Li Bihan[1,2], Wang Ruijun[1,2]

[1] Beijing Golden Wheel Special Machine Co., Ltd, Beijing 100083, China; [2] Chinese Academy of Agricultural Mechanization Sciences, Beijing 100083, China

Abstract: To improve the bonding strength of the chromium-doped diamond-like carbon (Cr-DLC) films on the surface of the copper alloy, multilayer structure films of Cr/CrN/Cr-DLC with different thickness of Cr interlayer were designed and prepared on the copper alloy samples by magnetron sputtering and plasma enhanced chemical vapor deposition. The microstructure, residual stress, nanohardness, elastic modulus, bonding strength and impact toughness of the film were tested by high-resolution Raman spectrometer, film stress meter, nanoindenter, scratch tester and repetitive impact tester. The results show that the residual stress of Cr-DLC film on the surface of copper alloy decreases from −1.92 GPa to −0.47 GPa with increasing the thickness of Cr interlayer, reduced by 75.5%. When the thickness of Cr interlayer reaches 1.01 μm, the bonding strength between the Cr-DLC film and the substrate is the best, which is 69% and 67% higher than the first (L_{c1}) and the second (L_{c2}) critical loads of Cr-DLC film without Cr adhesive layer, respectively. After 20 000 times of repetitive impact tests, there is no elastic recovery in the impact depth for all Cr-DLC coated samples, and exfoliation of a certain area for the film is observed at the center of the impact pit. Among all samples, Cr-DLC coated sample with Cr interlayer of 1.01 μm in thickness has the smallest peeling area, and shows the best performance of repetitive impact resistance. Therefore, Cr interlayer with a certain thickness can significantly reduce the residual stress of the Cr-DLC film while improve the bonding strength and repetitive impact resistance.

Key words: copper alloy; Cr interlayer; residual stress; adhesion; micro-impact tests

Chromium-doped diamond-like carbon films (Cr-DLC) prepared by physical vapor deposition (PVD) are widely used in protective coatings because of their excellent mechanical properties. Mechanical properties of hard thin films on soft metals such as copper and aluminum are strongly affected by working load and residual stress. To satisfy the functional requirements for different applications, the interlayer of Cr/CrN can be introduced into Cr-DLC multilayer films for controlling residual stress, improving the adhesion and increasing the thickness and impact toughness.

Films with a single layer are prone to severe brittle fracture or even peel off the substrate under heavy load. The hardness of single-layer films is not high, and the bearing capability is poor; when the substrate yields but the film does not yield and deform, it will break; the poor adhesion between the film and the substrate makes it easily to peel off the substrate; meanwhile, poor toughness of the film leads to the propagation of the crack along the cross section, as shown in Fig. 1, which shows the bearing capacity of single-layer and multilayer carbon based films. It is easy to find out that the multilayer structure improves the bearing capacity of the films[1-3].

The failure of hard thin films on soft substrates is caused by delamination and fracture[4], and is related to relatively high compressive residual stress and stress gradient. Residual stress in PVD films is mainly from thermal residual stress generated in deposition process, intrinsic stress of the films and the interaction between them[5-7]. Thermal residual stress is originated from the difference of thermal expansion between films and substrates during the process of cooling from deposition temperature to room temperature. For intrinsic stress generated in the deposition process, its density is depended on deposition conditions, such as reference potential on the substrate, distance between the working gas and the

Received date: April 02, 2021
Corresponding author: Wang Ruijun, Ph. D., Chinese Academy of Agricultural Mechanization Sciences, Beijing 100083, P. R. China, Tel: 0086-10-64882277, E-mail: 13701380963@163.com

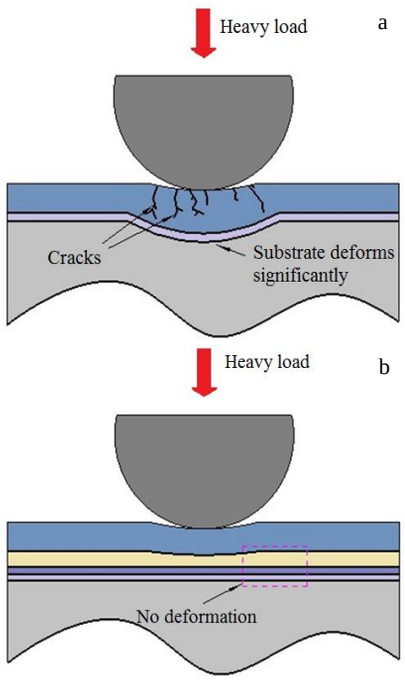

Fig.1 Schematic diagram of bearing capacity of single-layer (a) and multilayer (b) carbon based composite films

target, doping amount and film thickness. For PVD films, the effect of residual stress on the properties of PVD films can be effectively reduced by multilayer films under the premise that the target, gas and equipment are determined.

Multilayer structure with addition of metal or ceramics interlayer can improve interface adaptability and reduce the effect of residual stress. Metals of chromium and titanium are usually considered as the interlayer, and materials of the interlayer should have a thermal expansion coefficient similar to that of the substrate and also an elastic modulus similar to that of the carbon based film. It can effectively control the residual stress and improve adhesion between films and substrates by introducing multilayer structure such as the combination of metals and ceramics (Cr/CrN). Increase in the thickness of the metal layer can reduce the residual stress on surface, but may degrade the performance of multilayer films. Large plane residual stress is detected near the substrate when the thickness of CrN layer is relatively large, and concentrated columnar growth is found at the beginning, and finally the film fails due to the crack propagation. Therefore, an interlayer with a certain thickness is needed for each single CrN film. Metal Cr layer with an optimal thickness can further improve the adhesion and the toughness of multilayer films.

1 Experiment

1.1 Structure design for Cr-DLC film

A model of multilayer structure for Cr-DLC film was designed, and effects of hard film with metal interlayer on soft metals on internal stress and adhesion performance was investigated by varying thickness of Cr interlayer and keeping thickness of working layer constant. As shown in Fig. 2, a

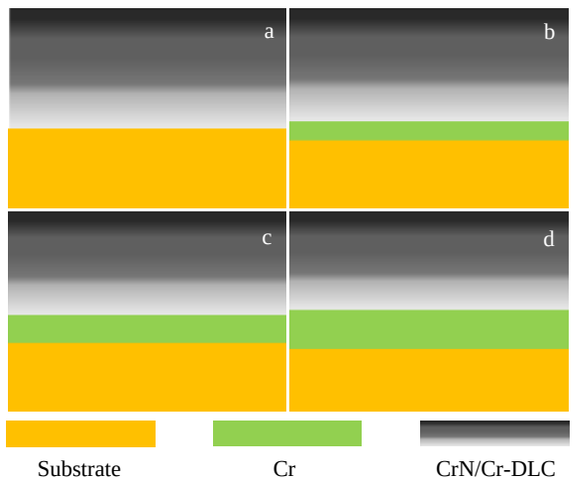

Fig.2 Multilayer structure model of Cr-DLC films: (a) Cr-DLC-1, (b) Cr-DLC-2, (c) Cr-DLC-3, and (d) Cr-DLC-4

working layer with 5 μm in thickness is prepared, the thickness of Cr interlayer changes from 0 μm to 1.5 μm, which is 0, 0.5, 1.0 and 1.5 μm for sample Cr-DLC-1, Cr-DLC-2, Cr-DLC-3 and Cr-DLC-4, respectively.

1.2 Film deposition

Films were prepared by multi-functional ion plating system. As shown in Fig. 3, unbalanced magnetron sputtering and plasma enhanced chemical vapor deposition can be both achieved by this system, equipped with two pairs of unbalanced magnetron sputtering targets and one rectangular anode layer gas ion source. The working gas is argon with 99.99% purity and methane with 99.99% purity.

*Φ*30 mm×5 mm samples of KK3 copper alloy were used as substrates, which were treated by polishing and had a surface roughness of 0.8 μm. These samples were subjected to multi-process ultrasonic cleaning for 30 min, and put into an 80 °C oven for drying after cleaning. The samples were placed in the vacuum chamber with a vacuum degree of 5×10^{-3} Pa. The oxide layer on surface of substrates was removed by plasma etching after introducing argon while the vacuum degree was 5×10^{-1} Pa, and film deposition begins when the vacuum degree reaches 3×10^{-1} Pa. The total gas pressure, the bias voltage and the etching time for plasma etching process were 1.0 Pa, −400 V and 30 min, respectively; process parameters for Cr interlayer with four different thicknesses are presented in Table 1.

1.3 Characterization

The microstructure of the film was measured and analyzed by LabRAM HR Evolution high resolution Raman spectrometer, 514 nm laser was used for exciting the film, the beam spot diameter was 1.25 μm, the power was 150 μW/cm^2, scanning time was 60 s, and accumulation time was once. S-4800 cold field emission scanning electron microscope was used to study cross section morphology and the film thickness. SuPro FST1000 film stress tester was used for detecting film deposited samples, and the testing parameters were: optical distance of 1024.8 mm, elastic modulus of 195

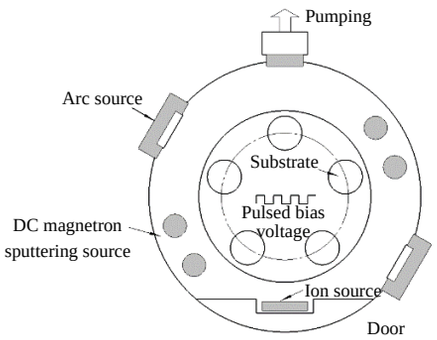

Fig.3 Multi-functional ion plating system

GPa, Poisson's ratio of 0.3 and sample thickness of 0.8 mm. The intrinsic stress of the deposited coating is given by Stoney's equation[8]:

$$\sigma = \frac{E_s h_s^2}{6(1-v_s)h_c}\left(\frac{1}{R}-\frac{1}{R_0}\right)$$

where E_s is the elastic modulus of the substrate; v_s is the Poisson's ratio of the substrate; h_s and h_c are the substrate and film thicknesses, respectively; R_0 and R are the radii of curvature of the substrate before and after deposition, respectively.

The adhesion force of film and substrate was tested by MFT-4000 multifunctional material surface performance tester, where the ending load was set at 100 N, the loading rate was 100 N/min, and the scratch length was 5 mm. The impact toughness of the film was measured by GP-100k continuous impact testing machine. WC ball with diameter of 5 mm was chosen as the punch. The distance between the punch and the sample was 1.0 mm, the impact frequency was 10 Hz, the load was 500 N, and the test cycle was 20 000 times. The scratch shape and impact pit morphology were observed by LY-WN-YH 3D full freedom microscopic imaging system. The coating hardness and Young's modulus were determined with a nano-indention testing system (Agilent G200). A fixed indentation depth of 400 nm was used to record the load after the maximum depth. At the same time, the significant influence on the hardness measured by the substrate was avoided. Each sample was indented 10 times to obtain the average value.

2 Results and Discussion

2.1 Microstructure of films

2.1.1 Structure

Fig. 4 illustrates Raman spectra of Cr-DLC films with different thicknesses of Cr interlayers. It is found that all of four samples have typical diamond-like carbon structure which has a D peak at 1350 cm^{-1} and an asymmetric G peak at 1580 cm^{-1}. The ratio of I_D/I_G can estimate the content of sp^3 hybrid bond, and lower ratio represents higher content of sp^3 hybrid bond. The G peak position, D peak position and the ratio of I_D/I_G for four Cr-DLC samples with different Cr interlayer thicknesses are illustrated in Table 2. It is concluded that all prepared samples have typical diamond-like carbon structure. All four samples have same working layers, in spite of the difference of I_D/I_G, where the ratio in the range of 0.46~0.50 can be ignored. The contents of sp^3 hybrid bond for four Cr-DLC samples with different Cr interlayer thicknesses are basically at the same level.

2.1.2 Thickness and microscopic structure

As shown in Fig. 5, thickness of four different Cr-DLC samples is 4.83, 4.91, 5.81 and 7.12 μm, respectively. And corresponding Cr interlayer thickness for samples Cr-DLC-1, Cr-DLC-2, Cr-DLC-3 and Cr-DLC-4 is 0, 0.65, 1.01 and 1.83 μm, respectively. It is basically consistent with the design

Table 1 Deposition parameters for Cr-DLC films

Sample	Coating process	Total gas pressure/Pa	Gas flow			Current/A	Bias/V	Time/min
			Ar	N_2	CH_4			
Cr-DLC-1	Plasma cleaning	1.0	170	-	-	-	600	35
	Cr layer	0.3	200	-	-	10	80	0
	CrN layer	0.3	200	60	-	15	80	32.5
	Cr-DLC	0.3	200	0	60~130	8	80	240
Cr-DLC -2	Plasma cleaning	1.0	170	-	-	-	600	35
	Cr layer	0.3	200	-	-	10	80	20
	CrN layer	0.3	200	60	-	15	80	32.5
	Cr-DLC	0.3	200	0	60~130	8	80	240
Cr-DLC -3	Plasma cleaning	1.0	170	-	-	-	600	35
	Cr layer	0.3	200	-	-	10	80	40
	CrN layer	0.3	200	60	-	15	80	32.5
	Cr-DLC	0.3	200	0	60~130	8	80	240
Cr-DLC -4	Plasma cleaning	1.0	170	-	-	-	600	35
	Cr layer	0.3	200	-	-	10	80	80
	CrN layer	0.3	200	60	-	15	80	32.5
	Cr-DLC	0.3	200	0	60~130	8	80	240

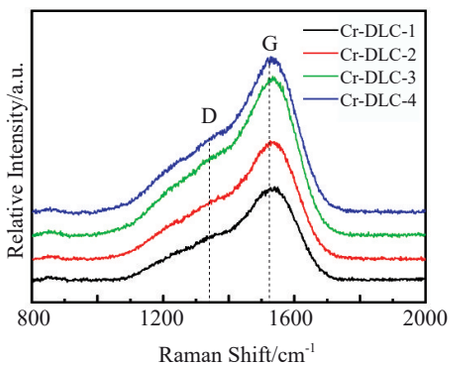

Fig.4 Raman spectra of the Cr-DLC films with different interlayers

Table 2 G peak, D peak and I_D/I_G of different samples

Samples	Position/cm^{-1}		Integral area/cm^{-2}		I_D/I_G
	D	G	D	G	
Cr-DLC -1	1347.5	1536.94	175931.25	384178.51	0.46
Cr-DLC -2	1326.91	1532	222174.37	484783.95	0.46
Cr-DLC -3	1340.91	1540.24	195865.13	416969.12	0.47
Cr-DLC -4	1359.03	1533.65	318486.88	635392.35	0.50

requirements. The cross section morphology shows that films of four samples are uniform and have compact structure and also well bonded between the film and the substrate, and no obvious spalling is observed.

2.2 Hardness and elastic modulus

Mechanical properties for Cr-DLC films are shown in Fig. 6. It can be concluded that the average hardness for Cr-DLC-1, Cr-DLC-2, Cr-DLC-3 and Cr-DLC-4 is 11.86, 11.46, 11.09 and 11.03 GPa, respectively, and the corresponding average elastic moduli are 135, 136, 143.8 and 148 GPa, respectively. The introduction of Cr interlayer increases the elastic modulus of films, but with increasing the thickness of Cr interlayer, the average hardness decreases due to its own low hardness.

2.3 Residual stress

The stress state for thin films is significant, which affects many properties, including adhesion between films and substrates, internal cracks, wear resistance, fatigue failure, stress corrosion and hardness. The residual stress caused by mismatch of thermal expansion for films and substrates and large temperature deviation between deposition temperature and operation temperature is called thermal stress[9-11]. Residual stress may also be caused by defects in the growth of films or defects introduced by films application, which is called intrinsic stress. For vacuum deposited films, intrinsic stress is the typical result of crystallization defects accumulated during the deposition process[12-16].

Fig. 7 shows the slope change of laser beam deflection distance-sample running distance (*L-D*) of samples before and after film deposition by Supro FST1000 film stress meter. Substitute the test data into the Stoney equation and the residual stress is shown in Table 3. The residual stress in four Cr-DLC samples is all compressive, which first decreases and then increases with increasing the thickness of Cr interlayer. The minimum residual stress is −0.47 GPa, decreased by 75.5%. There is little change in parameters for deposition process, resulting in little effect on intrinsic stress of films, so the difference of the residual stress is the variation of the thermal stress generated by Cr interlayer thickness. For sample Cr-DLC-1, absence of Cr interlayer leads to big difference of thermal expansion coefficient between CrN layer and the substrate and results in high thermal stress. Depositing

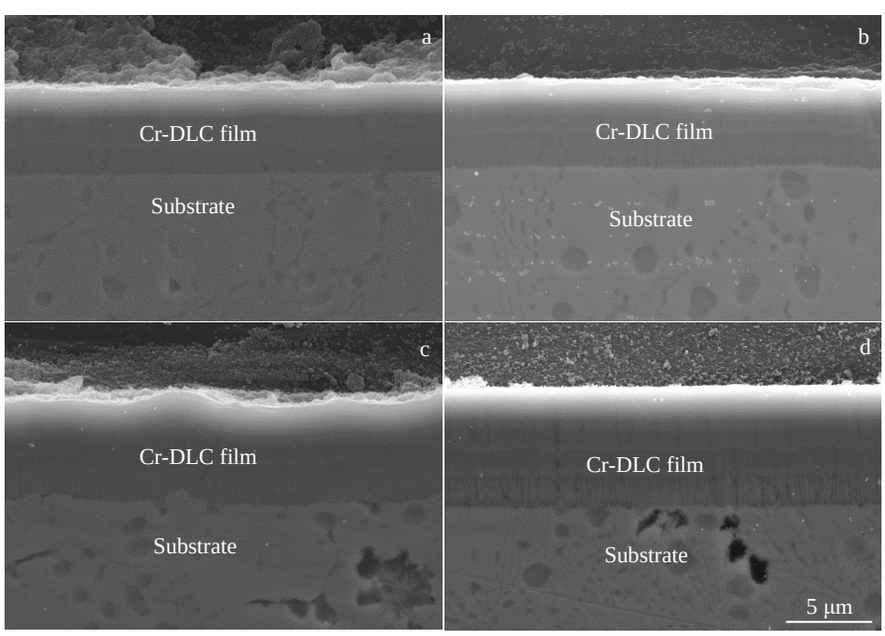

Fig.5 Thickness and cross section morphologies of Cr-DLC films with different interlayers: (a) Cr-DLC-1, (b) Cr-DLC-2, (c) Cr-DLC-3, and (d) Cr-DLC-4

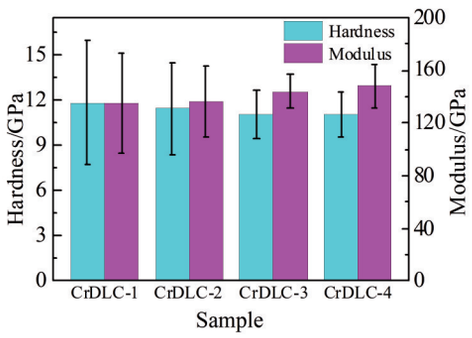

Fig.6 Intrinsic hardness and elastic modulus in multilayer configurations of Cr-DLC samples

Cr-DLC layer on Cr interlayer may generate less stress compared to depositing Cr-DLC layer directly on the substrate. Therefore, the introduction of Cr interlayer reduces the difference between the DLC film and the substrate, which decreases thermal stress of Cr-DLC and results in lower residual stress. This may prevent films from spalling from substrates. When increasing the thickness of Cr interlayer, more deposition time results in longer plasma etching, and leads to higher residual stress in films.

2.4 Adhesion

According to the standard of ASTM C1623-2005, the load at which the first crack appears in the film during a scratch test is considered as L_{c1}, and with increasing load, continuous film spalling occurs, it is considered as L_{c2}, which is the bonding strength between the film and the substrate. As shown in Fig.8, scratches of four Cr-DLC samples at L_{c1} can be observed by optical microscope. The first failure for all samples is a semicircular crack caused by buckling and the first delamination in the scratch track, which is quite a common failure for hard thin films on soft substrates such as KK3 alloy. The crack volume for Cr-DLC-1 sample is high, and it continues until the final delamination of multilayer structure. Due to the absence of Cr interlayer, the crack appears together with the eutectic crack of the intermediate nitride structure and reaches the substrate directly, which may be the reason for continuous spalling for the film under relatively low critical load. Other three samples show relatively high critical load for spalling because of the introduction of Cr interlayer, which absorbs more energy[17-20].

Fig.9 shows continuous film spalling. Combined with Fig.8, it can be found that in addition to spallation in the scratch track, the fine tensile stress crack in the buckling failure position-semicircular cracks is parallel to the trailing edge of the indenter, which reflects that the film is multilayer structure and still adheres to the substrate, and these cracks are generated from the balance between the tensile friction force from the trailing edge of the indenter and the compressive friction force from front edge of the indenter. This may be due to the high friction stress caused by the adhesion of Cr interlayer on the indenter. In addition, the friction between Cr interlayer and diamond indenter may also affect the critical load of multilayer films.

Fig.10 shows relationship between the adhesion strength at which the film is failed and the adhesion force between the film and the substrate. It is found that L_{c1} for sample Cr-DLC-1, Cr-DLC-2, Cr-DLC-3 and Cr-DLC-4 is 26, 29, 44 and 31 N, respectively. And corresponding L_{c2} is 30, 32, 50 and 37 N, respectively. Increasing thickness of Cr interlayer improves the adhesion between films and substrates, but when the

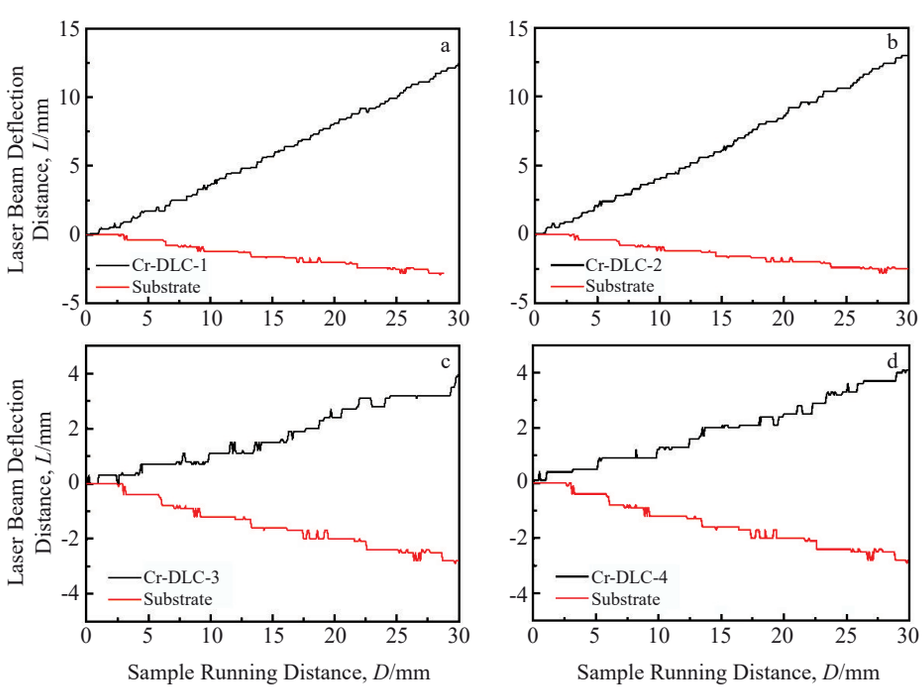

Fig.7 *L-D* relationships of Cr-DLC films with different interlayers: (a) Cr-DLC-1 (b) Cr-DLC-2 (c) Cr-DLC-3 (d) Cr-DLC-4

Table 3 Different interlayers of internal stress in multilayer configurations of Cr-DLC

Sample	Residual stress/GPa
Cr-DLC -1	−1.92
Cr-DLC -2	−1.52
Cr-DLC -3	−0.47
Cr-DLC -4	−0.63

interlayer reaches a certain thickness, the adhesion becomes poor due to reduced support of over thick interlayer and forms "eggshell effect". Results show the first critical load and the second critical load for Cr-DLC films with Cr interlayer is increased by 69% and 67%, respectively. Compared with Cr-DLC films without Cr interlayer, Cr-DLC shows the best performance when the thickness of Cr interlayer is 1.01 μm.

2.5 Repetitive impact test

As shown in Fig. 11, impact strongly affects four film deposited samples, and no elastic recovery is observed for impact depth at the impact pits of four samples after test [21-26]. At the center of the impact pits, there is a certain area of film spalling for four samples; Cr-DLC-1 has the largest area of spalling region, and Cr-DLC-2 and Cr-DLC-4 have a quite similar spalling area; the smallest area is observed for Cr-DLC-3, which represents the best repetitive impact resistance.

In the initial process of impact, the yielding stress of KK3 substrate is exceeded, impact depth increases with larger area of contact region, so the contact stress decreases due to plastic deformation. Multilayer structure of four kinds of Cr-DLC films shows good ability of deformation with the substrate, and no ring cracking is observed. When the contact area of the punch increases to the extent that the substrate no longer yields, the change in the depth of each continuous impact is the minimum. During each impact, films must bend significantly to accommodate the elastic and plastic deformation of the film, which increases the possibility of

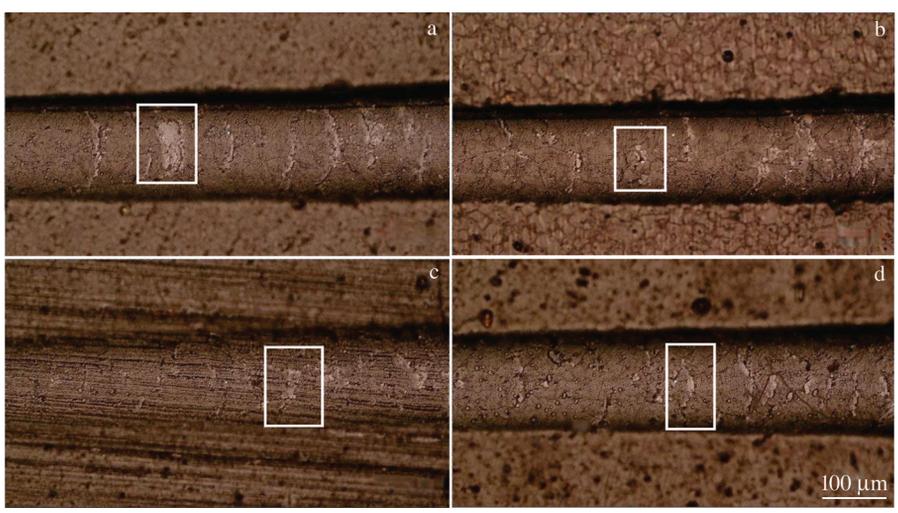

Fig.8 OM images of the first failure in Cr-DLC films with different interlayers: (a) Cr-DLC-1, (b) Cr-DLC-2, (c) Cr-DLC-3, and (d) Cr-DLC-4

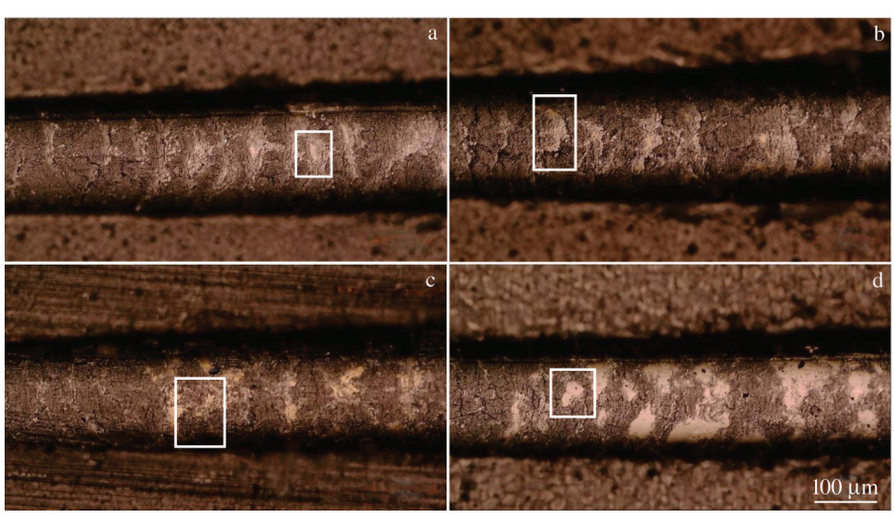

Fig.9 OM images showing continuous spalling failure of Cr-DLC films with different interlayers: (a) Cr-DLC-1, (b) Cr-DLC-2, (c) Cr-DLC-3, and (d) Cr-DLC-4

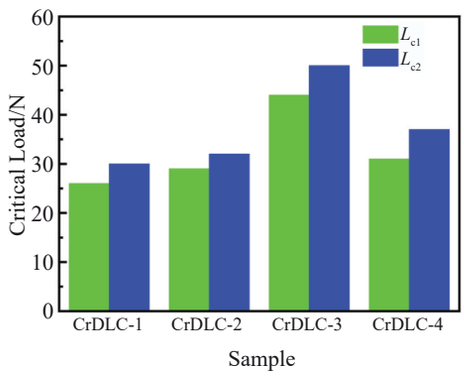

Fig.10 Critical scratch load for the first failure (L_{c1}) and complete failure (L_{c2}) of Cr-DLC film samples

cracking. As the hardness of Cr-DLC film is increased by 3~4 times compared with KK3 substrate, the depth decreases little with continuous impacts, which may be the beginning of the film damage. As the film is damaged by cracking, the impact depth increases further. There is no Cr interlayer for Cr-DLC-1, and its resistance against crack propagation is worse than other three samples. According to Fig. 11, the spalling area is decreased with increasing the thickness of Cr interlayer, which shows that internal stress is reduced constantly and the resistant ability against crack propagation is improved with increasing the thickness of Cr interlayer, finally resulting in less area of spalling region for films. As impact continues, the wear process becomes more obvious, including cracks through the thickness and large spalling debris, which eventually lead to film failure and substrate exposure around the impact pits.

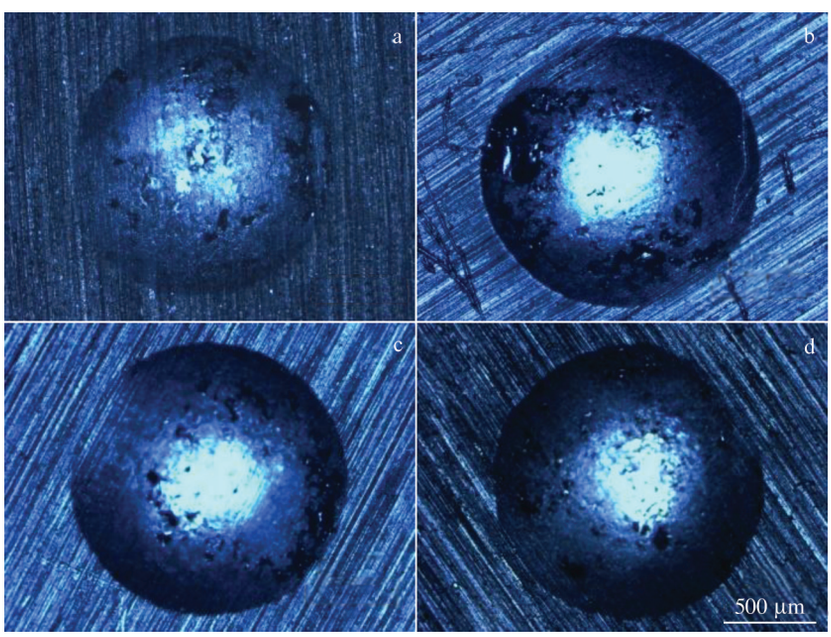

Fig.11 Morphologies of impact pits for repetitive impact tests after 20 000 times: (a) Cr-DLC-1, (b) Cr-DLC-2, (c) Cr-DLC-3, and (d) Cr-DLC-4

3 Conclusions

1) The hardness of Cr-DLC film decreases slightly with increasing the Cr interlayer thickness, but still remains above 11 GPa when the thickness of working layer keeps constant.

2) Compressive residual stress can be detected for four kinds of Cr-DLC films with different Cr interlayer thicknesses, and the stress first decreases and then increases with increasing the thickness of Cr interlayer. When the thickness of Cr interlayer is 1.01 μm, the residual stress decreases to −0.47 GPa, which has a reduction of 75.5%.

3) Films show better adhesion to the substrate as the Cr interlayer thickness increases. The first critical load and the second critical load of Cr-DLC films with Cr interlayer is improved by 69% and 67%, respectively compared with films without Cr interlayer, and Cr-DLC-3 film shows the best performance when the thickness of interlayer reaches 1.01 μm.

4) Repetitive impact strongly affects four kinds of samples. After the impact load is released, no elastic recovery can be observed for impact depth at the impact pits. At the center of the impact pits, a certain area of spalling can be found, and Cr-DLC-3 shows the least area of spalling, which represents the best resistance against repetitive impacts.

References

1 Holmberg K, Matthews A, Ronkainen H. *Tribology International* [J], 1998, 31(1-3): 107

2 Li Z D. *Study of Low Temperature Preparation and Properties of Long Life Thin Films on High Speed and Heavy Load Bearing* [D]. Beijing: Chinese Academy of Agricultural Mechanization Sciences, 2017 (in Chinese)

3 Zhan H. *Design and Preparation of Element Doping Carbon-*

based Thin Films for Marine Atmosphere Environment Applications[D]. Beijing: Chinese Academy of Agricultural Mechanization Sciences, 2018 (in Chinese)
4 Holmberg K, Ronkainen H, Laukkanen A *et al*. *Surface & Coatings Technology* [J], 2007, 202(4-7): 1034
5 Deng J, Manuel B. *Diamond and Related Materials*[J], 1996, 5: 478
6 Freund L B, Suresh S. *Thin Film Materials-Stress, Defect Formation and Surface Evolution*[M]. Cambridge: Cambridge University Press, 2004
7 Shao W, Zhou Y F, Shi Z J *et al. Materials Today Communications* [J], 2020, 23: 100 946
8 Stoney G G. *Proceedings of the Royal Society A*[J], 1909, 82: 172
9 Kenneth H, Helena R, Anssi L *et al. Wear*[J], 2009, 267: 2142
10 Karaseov P A, Podsvirov O A, Karabeshkin K V *et al*. *Nuclear Instruments and Methods in Physics Research B*[J], 2010, 268: 3107
11 Wang P, Wang X, Xu T *et al*. *Thin Solid Films*[J], 2007, 515: 6899
12 Oka Y, Kirinuki M, Nishimura Y *et al*. *Surface & Coatings Technology*[J], 2004,186: 141
13 Miki Y, Nishimoto A, Sone T *et al*. *Surface & Coatings Technology*[J], 2015, 283: 274
14 Lei Y, Jiang J L, Wang Y B *et al*. *Applied Surface Science*[J], 2019, 479: 12
15 Mei H J, Zhao S S, Chen W *et al*. *Trans Nonferrous Met Soc China*[J], 2018, 28: 1368
16 Baida H A, Kermouche G, Langlade C. *Mechanics of Materials* [J], 2015, 86: 11
17 Attar F, Johannesson T. *Surface and Coatings Technology*[J], 1996, 78: 87
18 Bull S J. *Tribology International* [J], 1997, 30(7): 491
19 Stallard J, Poulat S, Teer D G. *Tribology International*[J], 2006, 39: 159
20 Bull S J, Berasetegui E G. *Tribology International*[J], 2006, 39: 99
21 Beake B D, Goodes S R, Smith J F *et al*. *Diamond and Related Materials*[J], 2002,11: 1606
22 Sui X D, Liu J Y, Zhang S T *et al*. *Applied Surface Science*[J], 2018, 439: 24
23 Kermouche G, Grange F, Langlade C. *Materials Science & Engineering A*[J], 2013, 569: 71
24 Cinca N, Beake B D, Harris A J *et al*. *International Journal of Refractory Metals & Hard Materials*[J], 2019, 84: 105 045
25 Beake B D, Isern L, Endrino J L *et al*. *Wear*[J], 2019, 418-419: 102
26 Beake B D, Bird A, Isern L *et al*. *Thin Solid Films*[J], 2019, 688: 137 358

铜合金表面过渡层厚度对Cr-DLC薄膜残余应力和结合性能的影响

李振东[1,2]，詹　华[1,2]，徐天杨[1,2]，鲍曼雨[1,2]，李碧晗[1,2]，汪瑞军[1,2]
(1. 北京金轮坤天特种机械有限公司，北京 100083)
(2. 中国农业机械化科学研究院，北京 100083)

摘　要：为提高铜合金表面Cr-DLC薄膜的膜/基结合性能，设计了Cr/CrN/Cr-DLC多层结构薄膜，采用磁控溅射/等离子辅助气相沉积方法在铜合金样品表面制备不同Cr粘结层厚度的Cr掺杂类金刚石（Cr-DLC）薄膜。利用高分辨拉曼光谱仪、薄膜应力仪、纳米压痕仪、划痕仪和连续冲击试验机分别对薄膜的微观结构、残余应力、纳米硬度和弹性模量、薄膜与基体结合性能和耐冲击韧性进行测试。结果表明，随着Cr粘结层厚度的增加，铜合金表面Cr-DLC薄膜的残余应力出现了先升高后降低的趋势，最小残余应力达到−0.47 GPa，降幅高达75.5%。薄膜的膜/基结合力随Cr粘结层厚度的增加而提高，当Cr粘结层厚度为1.01 μm时，Cr-DLC薄膜的膜/基结合力最佳，与无Cr粘结层Cr-DLC薄膜的第1（L_{c1}）和第2（L_{c2}）临界载荷相比分别提高69%和67%。经20 000次连续冲击试验，所有薄膜样品冲击坑的冲击深度均没有弹性恢复，薄膜在冲击坑的中心位置均出现一定面积的剥落，其中，Cr粘结层厚度1.01 μm的Cr-DLC薄膜样品的膜层剥落面积最小，表现出了最好的抗连续冲击的能力。一定厚度Cr粘结层能够大幅降低铜合金表面Cr-DLC薄膜的残余应力，提高膜/基结合力和耐冲击性能。

关键词：铜合金；过渡层结构；残余应力；膜/基结合力；冲击试验

作者简介：李振东，男，1983年生，博士，高级工程师，中国农业机械化科学研究院，北京金轮坤天特种机械有限公司，北京 100083，电话：010-64883739，E-mail：18611903779@163.com